ARTICLES
PUBLISHED ONLINE: 16 MARCH 2014 | DOI: 10.1038/NCLIMATE2161
nature climate change

Sustained mass loss of the northeast Greenland ice sheet triggered by regional warming

Shfaqat A. Khan[1*], Kurt H. Kjær[2], Michael Bevis[3], Jonathan L. Bamber[4], John Wahr[5], Kristian K. Kjeldsen[2], Anders A. Bjørk[2], Niels J. Korsgaard[2], Leigh A. Stearns[6], Michiel R. van den Broeke[7], Lin Liu[8†], Nicolaj K. Larsen[9] and Ioana S. Muresan[1]

The Greenland ice sheet has been one of the largest contributors to global sea-level rise over the past 20 years, accounting for 0.5 mm yr^{-1} of a total of 3.2 mm yr^{-1}. A significant portion of this contribution is associated with the speed-up of an increased number of glaciers in southeast and northwest Greenland. Here, we show that the northeast Greenland ice stream, which extends more than 600 km into the interior of the ice sheet, is now undergoing sustained dynamic thinning, linked to regional warming, after more than a quarter of a century of stability. This sector of the Greenland ice sheet is of particular interest, because the drainage basin area covers 16% of the ice sheet (twice that of Jakobshavn Isbræ) and numerical model predictions suggest no significant mass loss for this sector, leading to an under-estimation of future global sea-level rise. The geometry of the bedrock and monotonic trend in glacier speed-up and mass loss suggests that dynamic drawdown of ice in this region will continue in the near future.

Mass loss from the Greenland ice sheet (GrIS) is regionally distributed between sectors manifesting quite different sensitivities to external forcings[1–3]. Enhanced surface melting and dynamic thinning associated with the speed-up of glacier flow[1] is mainly concentrated in the southest, west and northwest parts of the GrIS (refs 4–14), where most of the ice margin is in contact with the ocean. In southwest Greenland, where the ice sheet margin is typically located up to 100 km inland, there are few marine-terminating glaciers and mass loss is dominated by atmospheric forcing[1]. In contrast, major marine-terminating outlet glaciers characterize the northeast sector of Greenland, but these glaciers are surrounded by year-round sea ice, which suppresses calving front retreat[15].

Many of the glaciers in southeast, west and northwest Greenland that experienced dynamic thinning in 2003 and 2005, respectively, have somewhat slowed down in recent years[7,8,16]. However, the two glaciers with the largest contributions to GrIS mass loss—Jakobshavn Isbræ (JI) and Kangerdlugssuaq Glacier (KG)—have maintained their high rate of mass loss throughout the past decade[11] (Fig. 1a–c and Table 1). Both glaciers possess a negative bed slope[17,18] (a bed that deepens inland) that lies below sea level, the key conditions for satisfying the marine ice sheet instability hypothesis associated with parts of west Antarctica[19–21]. However, a far more substantive (by area) marine-based sector (Fig. 1) lies at the mouth of the >600-km-long northeast Greenland ice stream[22–24] (NEGIS), with its three main outlets, the Nioghalvfjerdsfjorden Glacier (NG) also called 79 North, the Zachariae Isstrøm (ZI) and Storstrømmen Glacier (SG) (Fig. 2a). NG is characterized by its almost 80-km-long and 20-km-wide floating tongue, widening to about 30 km at the calving front[22–26]. ZI has an almost 30-km-long calving front and is grounded at present. Both glaciers are located at the northeastern corner of the GrIS near Fram Strait and the Nordic Sea and are exposed to ocean variability[22]. They both have fast (>1 km yr^{-1}) near-terminus velocities. SG is located about 200 km south of ZI and has a 20-km-wide calving front. However, SG diverges into two lobes, one which calves directly into the ocean, whereas the other merges with Bistrup Glacier (BG). Both lobes have slow (∼100 m yr^{-1}) near-terminus velocities.

Here we use repeat measurements of surface elevation over the entire GrIS to estimate dynamic thinning at marine margins (Fig. 1a–c and Supplementary Section 1.0). Our results show that the NEGIS was relatively stable for at least a quarter of a century, followed by rapid dynamic thinning starting some time between 2003 and 2006. To investigate possible forcing mechanisms capable of triggering such instability, we analyse surface and subsurface water temperature, near-surface air temperature variations and sea ice concentrations.

We map elevation changes from April 2003 to April 2012 using altimeter surveys from the National Aeronautics and Space Administration's airborne topographic mapper (ATM) flights from 2003 to 2012 (ref. 27) supplemented with ice, cloud and land elevation satellite (ICESat) laser altimeter data from 2003 to 2009 (ref. 28), land, vegetation and ice sensor (LVIS) data from 2007 to 2012 (ref. 29) and European Space Agency Environmental Satellite (ENVISAT) data from April 2009 to March 2012 (ref. 30). To assess thinning before 2003, we produced a 25 × 25 m gridded digital elevation model using aerial photographs[31] from 1978 that cover the

[1]DTU Space, National Space Institute, Technical University of Denmark, Department of Geodesy, Kgs. Lyngby 2800, Denmark, [2]Centre for GeoGenetics, Natural History Museum of Denmark, University of Copenhagen, Copenhagen 1350, Denmark, [3]Geodetic Science, Ohio State University, Columbus, Ohio 43210, USA, [4]Bristol Glaciology Centre, University of Bristol, Bristol BS8 1SS, UK, [5]Department of Physics and Cooperative Institute for Research in Environmental Sciences, University of Colorado, Boulder, Colorado 80309, USA, [6]Department of Geology, University of Kansas, Lawrence, Kansas 66045, USA, [7]Institute for Marine and Atmospheric Research, Utrecht University, Utrecht 80005, The Netherlands, [8]Department of Geophysics, Stanford University, Stanford, California 94305, USA, [9]Department of Geoscience, Aarhus University, Aarhus 8000, Denmark. †Present address: Earth System Science Programme, The Chinese University of Hong Kong, Hong Kong, China. *e-mail: abbas@space.dtu.dk

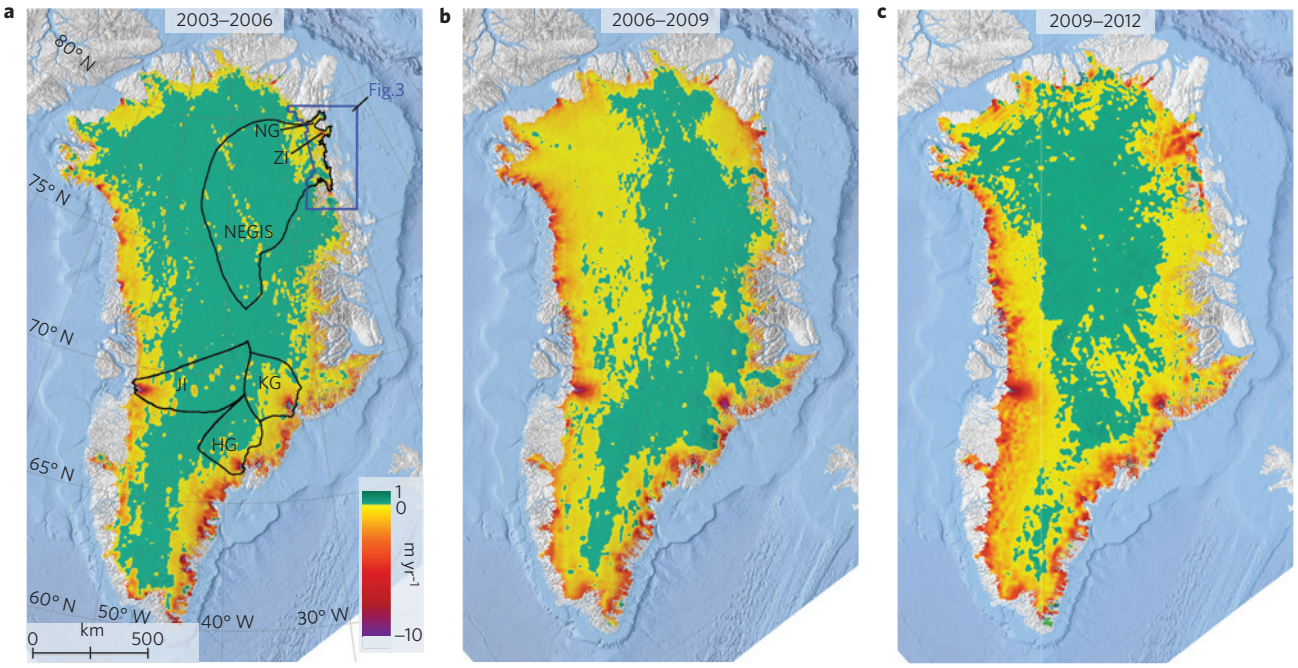

Figure 1 | Changes in surface elevations obtained using ICESat, ATM, LVIS and ENVISAT data (Supplementary Section 1.0). a–c, Ice surface elevation change rates in m yr^{-1} from April 2003 to April 2006 (**a**), April 2006 to April 2009 (**b**) and April 2009 to April 2012 (**c**).

Table 1 | Ice mass loss rates.

		Mass loss rate in Gt yr^{-1}			
Mass loss type	**Area**	**1978–2003**	**2003–2006**	**2006–2009**	**2009–2012**
SMB+dynamic	Coastal northeast GrIS	1.4 ± 26	4.3 ± 0.5	19.6 ± 0.6	20.2 ± 0.9
SMB+dynamic	NEGIS basin	-	−0.8 ± 1.6	11.7 ± 2.0	16.1 ± 3.7
SMB+dynamic	JG basin	-	10.4 ± 1.4	18.7 ± 1.2	27.4 ± 1.6
SMB+dynamic	KG basin	-	12.8 ± 0.9	11.1 ± 0.8	14.5 ± 1.0
SMB+dynamic	HG basin	-	4.9 ± 1.0	1.5 ± 0.9	2.9 ± 1.0
SMB	NEGIS basin	-	6.1 ± 0.9	0.5 ± 0.1	2.2 ± 0.3
SMB	JG basin	-	−1.3 ± 0.2	3.1 ± 0.4	10.9 ± 1.5
SMB	KG basin	-	0.1 ± 0.1	0.6 ± 0.1	3.9 ± 0.5
SMB	HG basin	-	−2.1 ± 0.3	3.0 ± 0.4	4.1 ± 0.6
Dynamic	NEGIS basin	-	−6.9 ± 1.8	11.2 ± 2.0	13.9 ± 3.7
Dynamic	JG basin	-	11.7 ± 1.4	15.6 ± 1.3	16.5 ± 2.2
Dynamic	KG basin	-	12.7 ± 0.9	10.5 ± 0.8	10.6 ± 1.1
Dynamic	HG basin	-	7.0 ± 1.0	−1.5 ± 1.0	−1.2 ± 1.2
SMB	GrIS	-	42.7 ± 6.6	151.7 ± 21.9	203.5 ± 29.4
Dynamic	GrIS	-	129.7 ± 22.7	140.3 ± 31.9	156.3 ± 40.9
SMB+dynamic	GrIS	-	172.4 ± 21.7	292.0 ± 23.2	359.8 ± 28.9
SMB+dynamic*	GrIS	-	205.0 ± 20.2	256.6 ± 21.8	363.5 ± 20.3
			2000–2010		
SMB+dynamic**	GrIS		211 ± 37		

Mass loss rates due to SMB and dynamically driven mass loss for coastal northeast GrIS shown in Fig. 3, NEGIS, JG, KG, HG and the GrIS rates are provided for April to April. * GRACE results from this study. ** Result of ice sheet mass balance exercise[6].

coastal portion of the northeast sector of Greenland (Fig. 2a and Supplementary Section 3.1).

Ice-sheet-wide mass loss

Mass loss rates calculated for the entire GrIS reveal a dramatic increase in loss caused by surface mass balance (SMB) between April 2003 and April 2012, and a complex contribution from dynamic mass loss (Table 1).

The average ice-sheet-wide mass loss increased from 172.4 ± 21.7 Gt yr^{-1} during April 2003–April 2006 to 359.8 ± 28.9 during April 2009–April 2012. The increase is due to a combination of increased dynamic mass loss and SMB-inferred mass loss. To

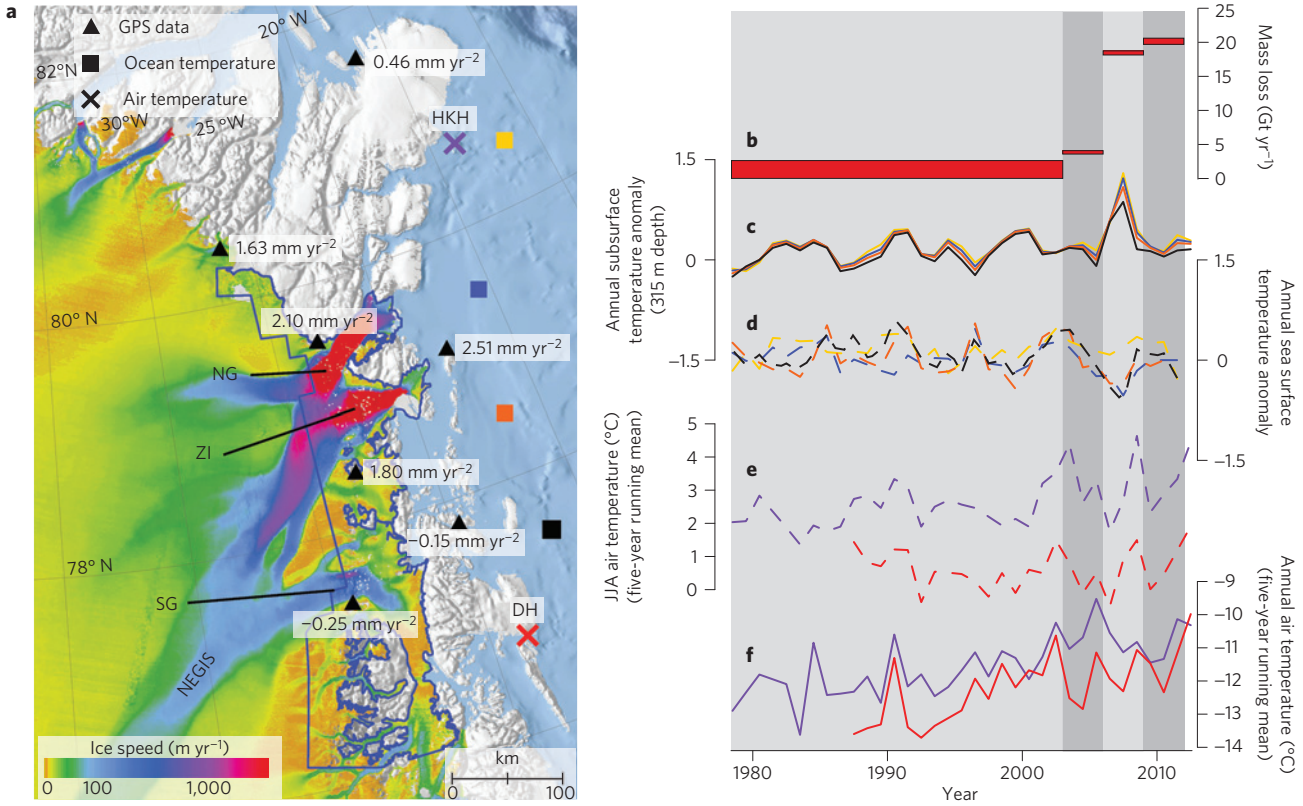

Figure 2 | Surface speed, mass loss rates and climate data. **a**, Colours indicate ice speed in m yr^{-1} during winter 2008–2009 (Supplementary Information). Triangles denote locations of GPS stations and their vertical accelerations in mm yr^{-2}. Squares and crosses denote locations of ocean and meteorological points, respectively. **b**, Ice mass rate from 1978 to 2012, grey shaded vertical bars represent three-year intervals (2003–2006, 2006–2009, 2009–2012) from April to April. **c**, Subsurface water temperature anomaly in °C after removing the 1961–1990 baseline. **d**, Sea surface temperature anomaly in °C after removing the 1961–1990 baseline. **e**, Mean summer air temperature in °C. JJA: June, July August. **f**, Red time series represents Danmarkshavn (DH), purple time series represents HKH, mean annual air temperature in °C. Each coloured line in **c**–**f** corresponds to a coloured square or cross in **a**.

estimate mass loss due to changes in ice dynamics, we subtract the SMB-inferred mass loss (obtained using the regional climate model RACMO2; ref. 32) from the observed mass loss rate. Dynamically driven mass loss rates increased from 129.7 ± 22.7 Gt yr^{-1} during April 2003–April 2006, to 156.3 ± 40.9 Gt yr^{-1} during April 2009–April 2012. This increase is mainly due to the acceleration of several outlet glaciers experiencing speed-up[4,5,8]. However, cases of glacier slowdown are reported[11], for example, at Helheim Glacier (HG) where dynamically driven mass loss decreased from 7.0 ± 1.0 Gt yr^{-1} during April 2003–April 2006, to −1.2 ± 1.2 Gt yr^{-1} during April 2009–April 2012. The other two main outlet glaciers in south Greenland, JI and KG, have kept their high rate of dynamically driven mass loss (>10 Gt yr^{-1}) throughout the past decade. In north Greenland, the NEGIS basin has increased its contribution to dynamically driven mass loss to more than 10 Gt yr^{-1} during April 2006–April 2012, a mass loss rate similar to JI after its speed-up in the late 1990s (ref. 33; Table 1). Estimation of ice flux rate for NG and ZI suggest an increase of ice flux by 9.8 ± 3.0 Gt yr^{-1} during February–April 2011 relative to winter 2000–2001. The flux rate for ZI increased further in 2012 (Supplementary Table 4).

Thinning of the northeast Greenland ice sheet since 1978

The average ice surface elevation change rates for coastal portions of the NEGIS between 1978 and 2003 are displayed in Fig. 3a. The 1978 digital elevation model, based on aerial photographs, is limited to areas below the snow line (within roughly 100 km of the ice margin), because the low contrast over snow prevents data sampling. To estimate elevation change rates between 1978 and 2003, we use aerial photography from 1978 and ICESat data from 2003. Figure 3a shows only minor elevation change rates during 1978–2003, suggesting this sector of the GrIS had been relatively stable for at least 25 years preceding 2003 (Table 1). This conclusion is further supported by sparse ATM data between 1995 and 1999 (Supplementary Section 3.1.2). Figure 3b shows that this stable period was followed by relatively localized fluctuations in elevation change rates during April 2003–April 2006. However, more pervasive and pronounced thinning rates are observed from April 2006 to April 2009 (Fig. 3c) and continue uninterrupted throughout April 2009–April 2012 (Fig. 3d). Thinning rates of more than 1 m yr^{-1} cover an area of 840 km^2 by April 2003–April 2006, 5,946 km^2 by April 2006–April 2009 and 7,747 km^2 by April 2009–April 2012. Figure 3e,f shows SMB-induced thinning rates for the same periods as in Fig. 3a–d. The thickening from 2003 to 2012 on SG and BG (two dome-like features located 60–100 km upstream from the main glacier flow line) is probably due to the buildup of mass in their reservoir area following the surges of the two glaciers during 1978–1984 (refs 34,35).

Accelerated mass loss associated with the NEGIS is further documented by continuous global positioning system (GPS) receivers established on bedrock to measure vertical surface displacement driven by the changes in ice loads[36]. All stations in the northeast sector of the Greenland GPS Network[37] are uplifting owing to some combination of the Earth's instantaneous elastic response to contemporary changes in ice mass and its delayed viscoelastic response to past changes in ice mass. However, accelerations in uplift can be attributed only to contemporary accelerations in ice mass losses. GPS data from 2008 to 2013

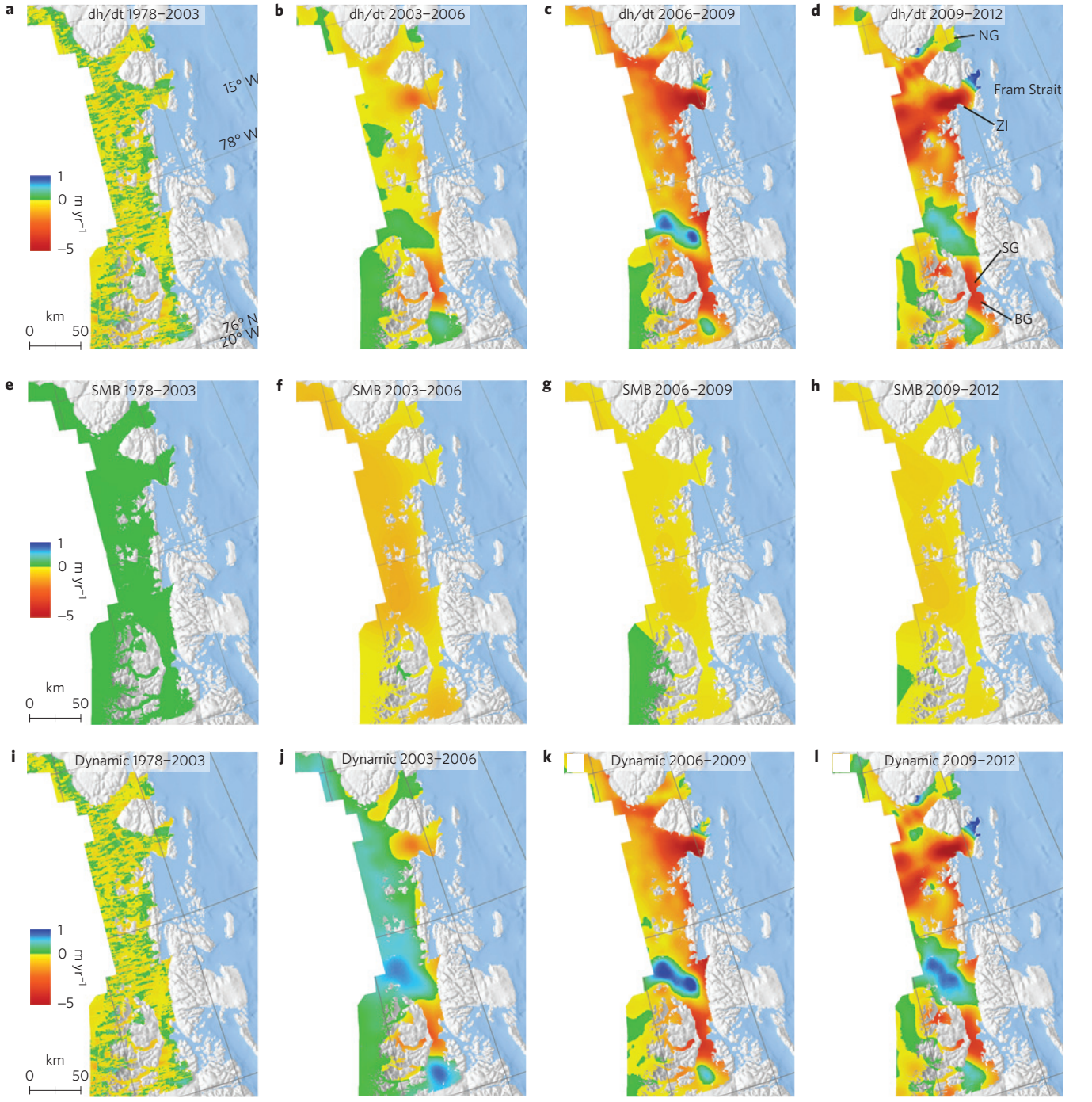

Figure 3 | Surface elevation change rates in northeast Greenland using aerial photographs, ICESat, ATM, LVIS and ENVISAT data. a–d, Observed ice surface elevation change rates in m yr^{-1} during August 1978–April 2003 (**a**), April 2003–April 2006 (**b**), April 2006–April 2009 (**c**) and April 2009–April 2012 (**d**). **e–h**, Total elevation change rates in m yr^{-1} owing to SMB fluctuations using regional climate model RACMO2 including firn compaction during August 1978–April 2003 (**e**), April 2003–April 2006 (**f**), April 2006–April 2009 (**g**) and April 2009–April 2012 (**h**). **i–l**, Dynamically driven elevation change rates in m yr^{-1} during August 1978-April 2003 (**i**), April 2003–April 2006 (**j**), April 2006–April 2009 (**k**) and April 2009–April 2012 (**l**).

record accelerating uplift (Fig. 2a) caused by increasing mass loss centered at the front of ZI. Combined with the elevation data this strongly supports the conclusion that ZI mass loss has been accelerating since at least 2003 and was ongoing through 2013.

Acceleration and retreat

Figure 4a,b shows positions of calving fronts at various times between 1978 and 2012. The 1978 calving front is obtained from aerial photos, whereas the 1999–2012 fronts are based on Land Remote-Sensing Satellite System images from http://glovis.usgs.gov and http://earthexplorer.usgs.gov. All images were recorded in July or August. The front of NG retreated by 5–7 km during 1978 and 2003, but was at more or less the same position between 2003 and 2009 (ref. 38). During 2009–2012 the southern tip and the mid-section retreated by 2–3 km. The retreat took place at the floating tip of the glacier. The frontal portion of ZI broke off during 2002. The break-off did not result in thinning, probably owing to low

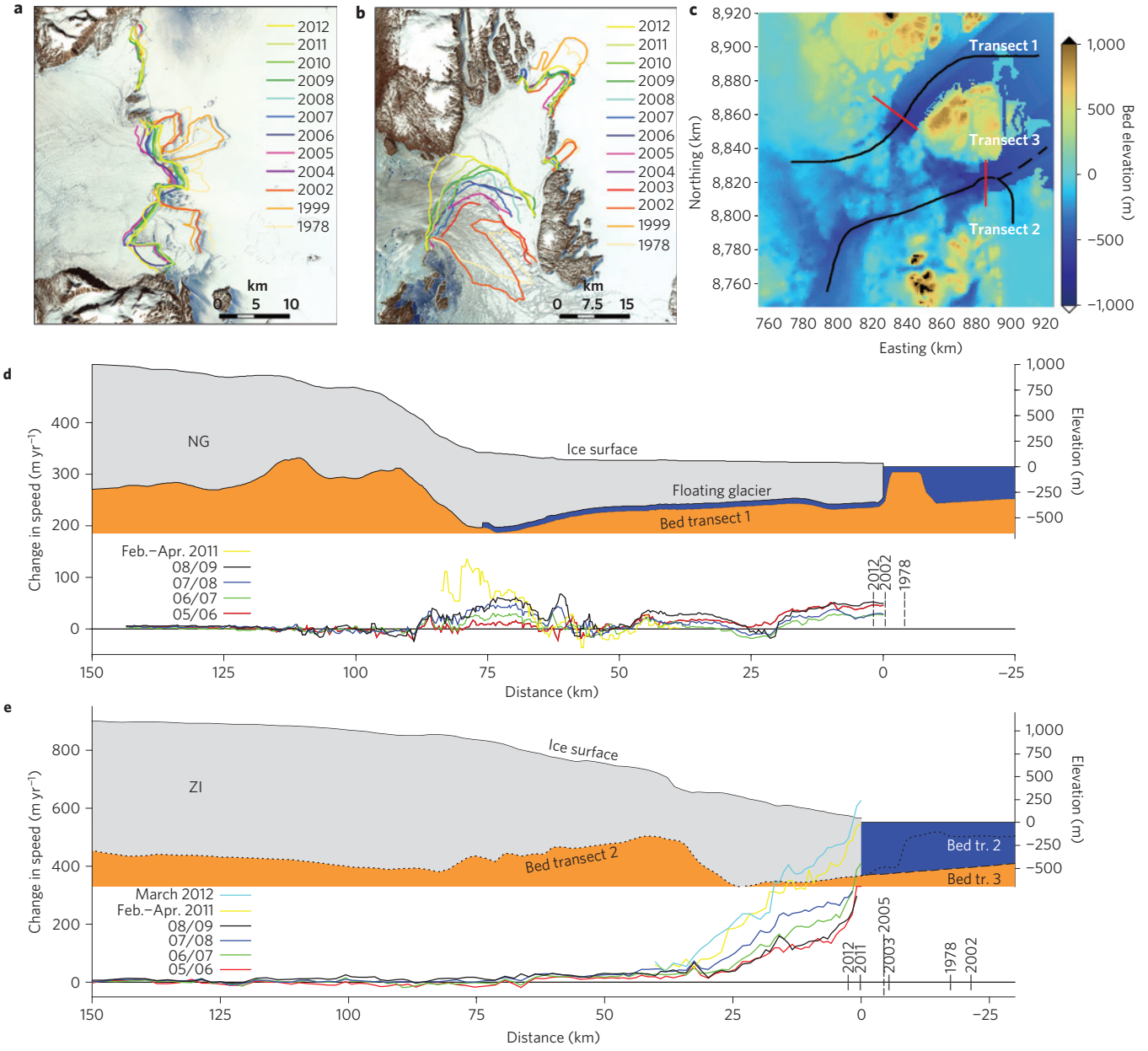

Figure 4 | Calving front positions, bed and velocity profiles along the main flow line of NG and ZI. a,**b**, Calving front positions of NG (**a**) and of ZI (**b**). **c**, Bed elevation in m. The solid lines denote main flow lines on NG and ZI. The dashed line denotes a transect from ZI's 2011 calving front in a northeast direction. Red lines denote flux gates locations. The axes display easting and northing coordinates in km for Universal Transverse Mercator zone 24. **d**, Top: bed and ice surface elevation above sea level along transect 1. Bottom: change in ice speed along transect 1 for various years relative to winter 2000/2001. **e**, Top: bed and ice surface elevation along transect 2. Bottom: change in ice speed for various years along transect 2.

lateral resistance[15]. The ZI retreated in 2002 and caused minor thinning near the front. However, once the portion of the glacier that is in deeper water (Fig. 4c) started to retreat in 2005–2006 (Fig. 4b), the thinning rate increased. The glacier continued retreating, thinning and speeding up with an accelerating rate through 2012.

To assess the dynamically induced thinning in northeast Greenland, we examine ice speeds during 2000–2012 along transect 1 and 2 (displayed as black lines in Fig. 4c). We use winter velocity maps for Greenland, derived using interferometric synthetic aperture radar (InSAR) data from the RADARSAT-1 satellite and the TerraSAR-X satellites, provided by the National Snow and Ice Data Center[39]. Changes in ice speeds during winter 2005–2006, winter 2006–2007, winter 2007–2008, winter 2008–2009, February–April 2011 and March 2012, relative to winter 2000–2001, are displayed in Fig. 4d,e. Bed and ice surface elevation above sea level[17] along transects 1 and 2 (displayed as black lines in Fig. 4c) are also shown in Fig. 4d,e. The two transects represent the main ice flow lines where the changes in ice speed are largest.

The floating tongue of NG increased its ice speed by 10–50 m yr^{-1} during 2005–2009 relative to the winter 2000–2001 ice speed (Fig. 4d) and by more than 100 m yr^{-1} in 2011 relative to winter 2000–2001. The calving front positions of NG and ZI in summer 2009 are located at a distance of 0 km for each transect plotted in Fig. 4d,e. Increased flow speeds of ZI started to migrate inland in winter 2008–2009 (Fig. 4e and Supplementary Fig. 14). During 2005–2006, 2006–2007 and 2008–2009 the winter speeds at

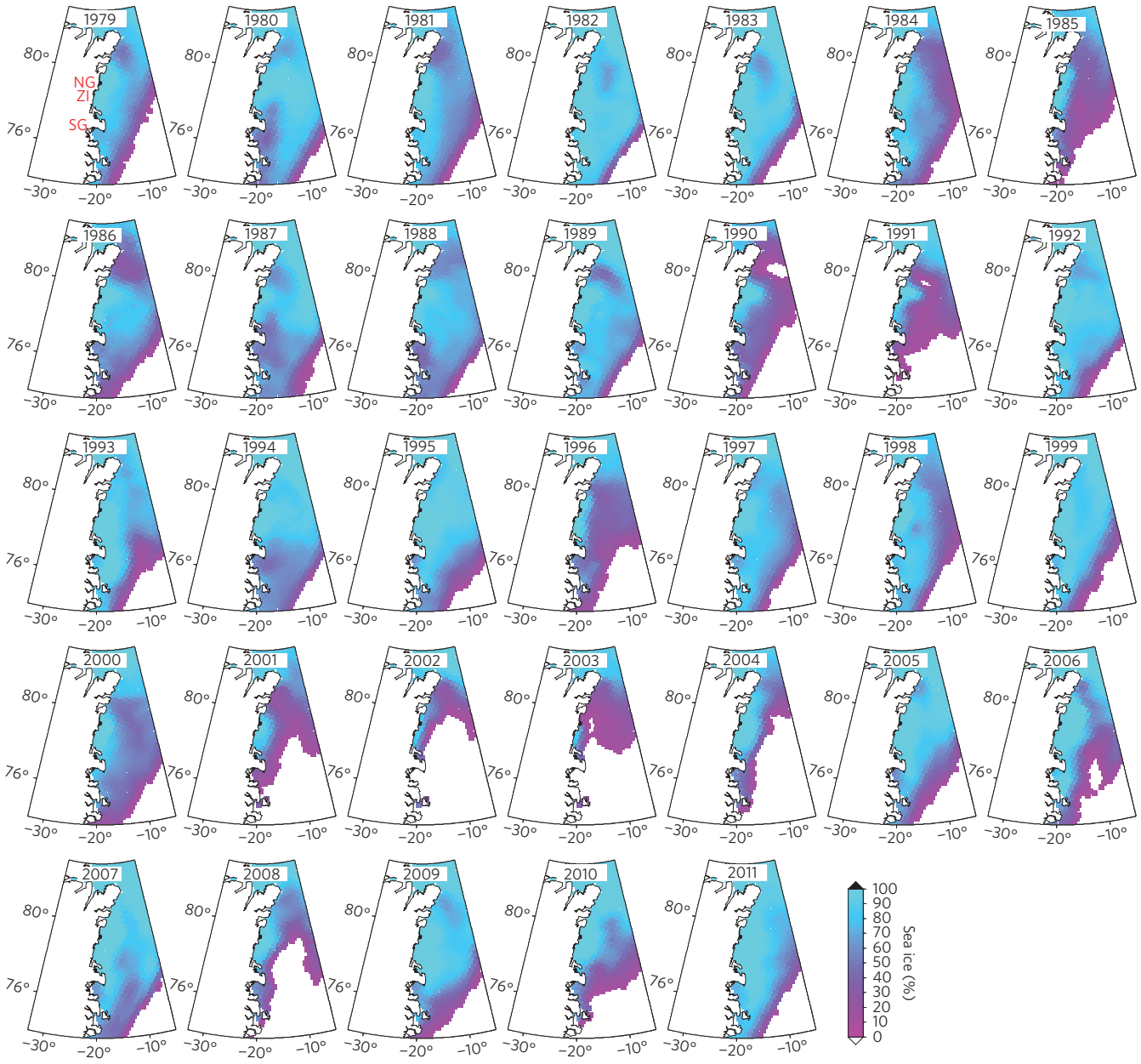

Figure 5 | Sea ice concentration along the northeast Greenland coast. Sea ice concentration (%) for September each year from 1979 to 2011. The sea ice grid resolution is 25 × 25 km.

distances above 70 km along the transect from Z1 to Z2 are more or less the same as that of winter 2000–2001. However, during winter 2008–2009 the speed at distances up to 150 km is larger than that of winter 2000–2001 (Supplementary Fig. 14). Velocities at the frontal portion of ZI resumed increase during February–April 2011 and suggest an increasing trend in velocity. However, it should be noted that we compare winter velocities. Summer velocities are likely to be larger.

Regional warming

Sea ice concentration for the month of September (typically the annual minimum) is displayed in Fig. 5 for 1979–2011. The data are derived using measurements from the Scanning Multichannel Microwave Radiometer on the Nimbus-7 satellite and from the Special Sensor Microwave/Imager sensors on the Defense Meteorological Satellite Program's -F8, -F11 and -F13 satellites[40]. The lowest monthly sea ice concentration in the fjord system located outside NG and ZI is observed in 2003, which probably caused the minor fluctuations in elevation change rates during April 2003–April 2006.

Annual mean sea surface temperature anomalies (Fig. 2d and Supplementary Information) show an increase in 2003, which coincides with the record low sea ice concentration in that year. Figure 2e,f shows the five-year running mean annual and summer (June–August) near-surface air temperature at Henrik Krøyer Holme (HKH) and Danmarkshavn. Both weather stations are located at the coast close to sea level[41]. Summer temperatures increased by about 2 °C in 2003 (Fig. 2e) compared with 1978. The high summer temperatures probably helped to reduce the sea ice extent, causing a retreat of about 10 km of the ZI calving front around 2002–2003 (Fig. 4e), which reduced the back stress acting on the floating fronts of the glacier. The absence of sea ice was accompanied by changes in glacier elevation rates near the margin (Fig. 2b).

During 1978–2003, annual mean subsurface water temperature anomalies (Supplementary Section 4.1) were 0.0°–0.3 °C higher than the 1961–1990 average (Fig. 2c). Inflow of large volumes of warmer water (0.5–0.8 °C) occurred about 2006–2007 (refs 42,43), which probably enhanced the sea ice retreat and glacier thinning rate (Fig. 2).

Conclusions

Our analysis suggests that increased air temperature (spike in Fig. 2e) triggered the dynamically induced mass loss around 2003. The warm summer temperatures probably reduced sea ice concentration in 2002–2004 (Fig. 5) causing both glacier fronts to calve heavily and retreat around 2002–2004 (Fig. 4a,b). This reduced the back stress acting on the lower glaciers and caused acceleration that propagated upstream (Fig. 4d,e). A combination of the reduced longitudinal stress and the reduced effective pressure due to thinning increased the driving stress as the glacier surface steepened. Retreat back into deeper water along the initially reverse-sloping bed allowed the calving rate to increase as a positive feedback. Entry of warm subsurface ocean water enhanced submarine melting and contributed further instability near the grounding line. Fig. 1 and Table 1 suggest that mass loss from the NEGIS has continued at a rate of $>10\,\mathrm{Gt\,yr^{-1}}$ even after a recovery in sea ice concentration and the intrusion of colder subsurface water from the east Greenland current into the fjord systems. This implies continued mass loss and frontal retreat until the NEGIS can reach a new equilibrium force balance (possibly until 25 km upstream from the 2012 calving front location where the bed slope reverses). The most recent predictions of mass loss from Greenland show no or only minor dynamically driven mass loss in the NEGIS basin, the largest in Greenland[44–46]. As recent model projections suggest, ocean warming around Greenland may reach almost double the global mean by 2100[47] and the recent assessment report of snow, water, ice and permafrost in the Arctic[48] projects the largest and most pronounced air temperature increase over northeast Greenland[48], increasing the risk of continued mass loss from this sector of Greenland.

Methods

Full Methods and associated references are available in the Supplementary Information.

Received 28 October 2013; accepted 4 February 2014; published online 16 March 2014

References

1. Van den Broeke, M. *et al.* Partitioning recent greenland mass loss. *Science* **326,** 984–986 (2009).
2. Holland, D. M., Thomas, R. H., De Young, B., Ribergaard, M. H. & Lyberth, B. Acceleration of Jakobshavn Isbræ triggered by warm subsurface ocean waters. *Nature Geosci.* **1,** 659–664 (2008).
3. Thomas, R. H. *et al.* Investigation of surface melting and dynamic thinning on Jakobshavn Isbræ, Greenland. *J. Glaciol.* **49,** 231–239 (2003).
4. Rignot, E., Box, J. E., Burgess, E. & Hanna, E. Mass balance of the Greenland ice sheet from 1958 to 2007. *Geophys. Res. Lett.* http://dx.doi.org/10.1029/2008GL035417 (2008).
5. Pritchard, H. D., Arthern., R. J., Vaughan, D. G. & Edwards, L. A. Extensive dynamic thinning on the margins of the Greenland and Antarctic ice sheets. *Nature* **461,** 971–975 (2009).
6. Shepherd, A. *et al.* A reconciled estimate of ice-sheet mass balance. *Science* **338,** 1183–1189 (2013).
7. Kjær, K. H. *et al.* Aerial photographs reveal late-20th-century dynamic ice loss in northwestern Greenland. *Science* **337,** 569–573 (2012).
8. Moon, T., Joughin, I., Smith, B. & Howat, I. 21st-century evolution of Greenland outlet glacier velocities. *Science* **336,** 576–578 (2012).
9. Stearns, L. A. & Hamilton, G. S. Rapid volume loss from two east Greenland outlet glaciers quantified using repeat stereo satellite imagery. *Geophys. Res. Lett.* **34,** L05503 (2007).
10. Luckman, A., Murray, T., de Lange, R. & Hanna, E. Rapid and synchronous ice-dynamic changes in east Greenland. *Geophys. Res. Lett.* **33,** L03503 (2006).
11. Howat, I. M. *et al.* Mass balance of Greenland's three largest outlet glaciers, 2000–2010. *Geophys. Res. Lett.* **38,** L12501 (2011).
12. Motyka, R. J., Fahnestock, M. & Truffer, M. Volume change of Jakobshavn Isbræ, West Greenland: 1985–1997–2007. *J. Glaciol.* **56,** 635–646 (2010).
13. Bjørk, A. A. *et al.* An aerial view of 80 years of climate-related glacier fluctuations in southeast Greenland. *Nature Geosci.* **5,** 427–432 (2012).
14. Khan, S. A. *et al.* Elastic uplift in southeast Greenland due to rapid ice mass loss. *Geophys. Res. Lett.* **34,** L21701 (2007).
15. Nick, F. M. *et al.* The response of Petermann Glacier, Greenland, to large calving events, and its future stability in the context of atmospheric and oceanic warming. *J. Glaciol.* http://dx.doi.org/10.3189/2012JoG11J242 (2012).
16. Sasgen, I. *et al.* Timing and origin of recent regional ice-mass loss in Greenland. *Earth Planet. Sc. Lett.* **333–334,** 29–303 (2012).
17. Bamber, J. L. *et al.* A new bed elevation dataset for Greenland. *Cryosphere* **7,** 499–510 (2013).
18. Joughin, I. *et al.* Seasonal to decadal scale variations in the surface velocity of Jakobshavn Isbrae, Greenland: Observation and model-based analysis. *J. Geophys. Res.* **117,** F02030 (2012).
19. Thomas, R. H. The dynamics of marine ice sheets. *J. Glaciol.* **24,** 167–177 (1979).
20. Weertman, J. Stability of the junction of an ice sheet and an ice shelf. *J. Glaciol.* **13,** 3–11 (1974).
21. Schoof, C. Ice sheet grounding line dynamics: Steady states, stability and hysteresis. *J. Geophys. Res.* **112,** F03S28 (2007).
22. Reeh, N., Thomsen, H., Higgins, A. K. & Weidick, A. Sea ice and the stability of north and northeast Greenland floating glaciers. *Ann. Glaciol.* **33,** 474–480 (2001).
23. Joughin, I., Fahnestock, M., MacAyeal, D., Bamber, J. L. & Goginensi, P. Observation and analysis of ice flow in the largest Greenland ice stream. *J. Geophys. Res.* **106,** 34021–34034 (2001).
24. Thomsen, H. H. *et al.* The Nioghalvfjerdsfjorden Glacier project, north–east Greenland: A study of ice sheet response to climatic change. *Geol. Greenland Survey Bull.* **176,** 95–103 (1997).
25. Seroussi, H. *et al.* Ice flux divergence anomalies on 79 North Glacier, Greenland. *Geophys. Res. Lett.* **38,** L09501 (2011).
26. Rignot, E. J. *et al.* North and northeast Greenland ice discharge from satellite radar interferometry. *Science* **276,** 934–937 (1997).
27. Krabill, W. B. *IceBridge ATM L2 Icessn Elevation, Slope, and Roughness, [1993–2012]. Boulder, Colorado, USA* (NASA Distributed Active Archive Center at the National Snow and Ice Data Center, 2012) http://nsidc.org/data/ilatm2.html.
28. Zwally, H. J. *et al. GLAS/ICESat L2 Antarctic and Greenland Ice Sheet Altimetry Data V031. Boulder, Colorado* (NASA Distributed Active Archive Center at the National Snow and Ice Data Center, 2011).
29. Blair, B. & Hofton, M. *IceBridge LVIS L2 Geolocated Ground Elevation and Return Energy Quartiles, Boulder, Colorado USA* (NASA Distributed Active Archive Center at the National Snow and Ice Data Center, 2012) http://nsidc.org/data/ilvis2.html.
30. ESA *ENVISAT RA2/MWR Product Handbook* (European Space Agency, 2007).
31. GST *Ground control for 1:150,000 scale aerials, Greenland* (Danish Ministry of the Environment, Danish Geodata Agency, 2013) http://www.gst.dk/Emner/Referencenet/Referencesystemer/GR96/.
32. Ettema, J. *et al.* Climate of the Greenland ice sheet using a high-resolution climate model–Part 1: Evaluation. *Cryosphere* **4,** 511–527 (2010).
33. Joughin, I., Abdalati, W. & Fahnestock, M. Large fluctuations in speed on Greenland's Jakobshavn Isbræ glacier. *Nature* **432,** 608–610 (2004).
34. Reeh, N., Bøggild, C. E. & Oerter, H. Surge of Storstrømmen, a large outlet glacier from the inland ice of north-east Greenland. *Grønl. Geol. Unders. Rapp.* **162,** 201–209 (1994).
35. Thomas, R., Frederick, E., Krabill, W., Manizade, S. & Martin, C. Recent changes on Greenland outlet glaciers. *J. Glaciol.* **55,** 147–162 (2009).
36. Khan, S. A., Wahr, J., Bevis, M., Velicogna, I. & Kendrick, E. Spread of ice mass loss into northwest Greenland observed by GRACE and GPS. *Geophys. Res. Lett.* **37,** L06501 (2010).
37. Bevis, M. *et al.* Bedrock displacements in Greenland manifest ice mass variations, climate cycles and climate change. *Proc. Natl Acad. Sci. USA* **109,** 11944–11948 (2012).
38. Box, J. E. & Decker, D. T. Greenland marine-terminating glacier area changes: 2000–2010. *Ann. Glaciol.* **37,** 91–98 (2011).
39. Joughin, I., Smith, B. E., Howat, I. M., Scambos, T. A. & Moon, T. Greenland flow variability from ice-sheet-wide velocity mapping. *J. Glaciol.* **56,** 415–430 (2010).
40. Comiso, J. *Bootstrap Sea Ice Concentrations from Nimbus-7 SMMR and DMSP SSM/I-SSMIS. Version 2. Boulder, Colorado USA* (NASA DAAC at the National Snow and Ice Data Center, 1999) updated 2012.

41. Cappelen, J. *Weather Observations from Greenland 1958–2012* Technical Report 13–11 (Ministry of Climate and Energy, 2012).
42. Ingleby, B. & Huddleston, M. Quality control of ocean temperature and salinity profiles–historical and real-time data. *J. Mar. Syst.* **65,** 158–175 (2007).
43. Beszczynska-Moller, A., Fahrbach, E., Schauer, U. & Hansen, E. Variability in Atlantic water temperature and transport at the entrance to the Arctic Ocean. *ICES J. Mar. Sci.* **69,** 1997–2010 (2012).
44. Nick, F. *et al.* Future sea-level rise from Greenland's main outlet glaciers in a warming climate. *Nature* **497,** 235–238 (2013).
45. Price, S. F., Payne, A. J., Howat, I. M. & Smith, B. E Committed sea-level rise for the next century from Greenland ice sheet dynamics during the past decade. *Proc. Natl Acad. Sci. USA* **108,** 8978–8983 (2011).
46. Gillet-Chaulet, F. *et al.* Greenland ice sheet contribution to sea-level rise from a new-generation ice-sheet model. *Cryosphere* **6,** 1561–1576 (2012).
47. Yin, J. *et al.* Different magnitudes of projected subsurface ocean warming around Greenland and Antarctica. *Nature Geosci.* **4,** 524–528 (2011).
48. AMAP, *The Greenland Ice Sheet in a Changing Climate: Snow, Water, Ice and Permafrost in the Arctic* (*SWIPA*) (Arctic Monitoring and Assessment Programme, 2011).

Acknowledgements

S.A.K., K.H.K. and I.S.M. were supported by the Danish Research Council (FNU). K.H.K. acknowledges support from Danish National Research Foundation (DNRF94-GeoGenetics). N.K.L. acknowledges support from the Danish Research Council no. 272-09-0095 and the VILLUM Foundation.

Author contributions

S.A.K. led the writing of the paper and conceived the study. S.A.K. analysed ENVISAT, ICESat, ATM, LVIS data surface and subsurface ocean temperatures. S.A.K. analysed GPS data. J.W. analysed GRACE data. A.A.B. analysed air temperature and glacier front positions. M.R.v.d.B. analysed SMB data. N.J.K. analysed 1978 aerial photographs. All authors contributed to data interpretation and writing of the manuscript.

Additional information

Supplementary information is available in the online version of the paper. Reprints and permissions information is available online at www.nature.com/reprints. Correspondence and requests for materials should be addressed to S.A.K.

Competing financial interests

The authors declare no competing financial interests.